Two-photon excited laser scanning confocal microscopy.

Diploma Paper
by
Per Petersson

Lund Reports on Atomic Physics, LRAP-226
November, 1997

Contents.

Abstract:

A comparison between two-photon and one-photon induced laser scanning spectroscopy has been made on a newly installed confocal microscope supplied by the BioRad microscopy division. The potential of the system combined with an optical multichannel analyser system (OMA) have been indicated by using an integrated set-up in tissue fluorescence studies. The puls width has been measured after passing through the microscope. A direct comparison between three optional photo-sensitisers used in photodynamic therapy has been made by studying the distribution of the fluorophores in cryo-cut sections of rat tumours. Some limitations of the system in the application of tissue fluorescence detection have hereby been high-lighted. An attempt to estimate the two-photon crossection of the three photo-sensitisers examined by quantifying the fluorescence signals and using Rhodamine B as a reference was made.

Introduction.

The microscope has indisputably changed the way we view biological science profoundly since good light microscopes became an available tool of investigation in the early part of the nineteenth century. A typical animal cell is 10 to 20 μm, which is about five times smaller than the smallest particle visible to the naked eye. In 1838 Schleiden and Schwann proposed that all plant and animal tissues are aggregates of individual cells, a theory that came to be known as the 'cell doctrine' and marked the formal birth of cell biology. Unfortunately animal cells turned out to be not only tiny, they are also colourless and translucent. Consequently the discovery of their internal features depended on the development of a variety of stains that provided sufficient contrast to make those features visible. The continuos search for improvements in microscopy has led to development of many types of microscopes, with the guiding development principal being that any new microscope should provide a visual source of information about objects that are otherwise too small to see with unaided eye. It is impossible to overlook the importance of such visual information, as our own sense of vision provides us with most of our information of the outside world. Further, the study of the interaction of light with molecules has been and continues to be of major importance in chemistry - molecular absorption spectroscopy has become one of the main analytical tools of the chemist and optical spectroscopy has contributed to the understanding of molecular structure and reactivity in a decisive way. These analyses are normally made on a macroscopic scale but the potential for the methods in applied microscopy is quite obvious.

This thesis focus is the technique of laserinduced fluorescence (LIF) in confocal laser scanning microscopy, primarily a comparison of two-photon induced excitations with UV single-photon excitations in examining tissue samples with the aim of distinguishing fluorescence properties of malignant tumours from normal tissue.

With fluorescence microscopy it is also possible to examine thicker light absorbing or light scattering objects, e.g. in *in vivo* studies in biological applications. In these studies fluorescence microscopy is most often used to detect specific proteins or molecules in cells and tissues, and a very powerful and widely used technique is to couple fluorescent dyes to antibody molecules, which then serve as highly specific and versatile staining reagents that bind selectively to the particular macromolecules that they recognise in cells or in extracellular matrix. But as the fluorescence spectrum, arising from auto fluorescence in the sample, itself contains a great deal of spectroscopic information added dyes are not always wanted. New methods even enable fluorescence microscopy to be used to

monitor changes in concentration and location of specific molecules inside living cells in real time.
Fluorescence microscopy requires a powerful light source and when laser became commercially available this was a natural step of improvement of the technique, the laser has also the extra advantage of freedom to pick one suitable excitation wavelength without losing light intensity.
The confocal arrangement provides a way to achieve optical sectioning of the scanned object , and thereby an opportunity to do 3D-scans of a thicker object and even reconstruct 3D-images of the object with computer image processing if desired.
Two-photon excitation occurs when extremely high light intensities are used for excitation, this offers some improvements to the conventional confocal microscopy technique and will be further discussed below.

Theory.

Fluorescence

Before discussing how the fluorescence spectrum can be used as a source of information we shall consider the phenomenon a bit more closely.
As an electromagnetic wavepacket, a photon, interacts with an atom or a molecule one of a few different possible outcomes is to be expected. If it exists a higher energetic state with an energy difference exactly corresponding to that of the incoming photon the molecule or atom can be excited up into this higher final state from it's initial ground state, that is the photon is **absorbed.** If, however, there is no higher state matching the incident frequency ($E=h\nu$), some of the energy may still be removed and subsequently reemitted in some direction in a process known as **elastic** or **coherent scattering**, because there is a phase relationship between the incident and scattered fields.
Picture the atom as a nucleus surrounded by an electron cloud (and the equivalent in the case of a molecule). The alternating **E**-field of the incoming lightwave will then impart energy to the atom as it drives the electron cloud into an oscillating motion. As the electron cloud starts vibrating with respect to the positive nucleus the system constitutes an oscillating dipole and will therefor start radiating with a frequency identical to that of the incoming lightwave, but the atom remains in it's ground state all along. The closer the frequency of the incoming light is to a resonance energy level, i.e. matching the energy gap up to the higher energy level, the more of the initial wave's energy will be scattered and carried off in the reemitted wave. If the frequency happens to match identically the photon is very

likely to be absorbed and then reradiated. This process, **resonance radiation**, isn't necessarily instantaneous like the elastic non-resonant scattering, but even if the photon is sent off in a random direction with a new polarisation it's total energy will be unaltered.
It is not hard to imagine that the problem of calculating the energy levels of a molecule is a lot more complex than for a single atom. The total angular momentum of the electrons in a molecule is not a constant of motion since the electrons do not move in a central field and the coupling of angular momenta for the electrons will therefore be different from that of the atom. An exception is the molecules which have axial symmetries, e.g. diatomic molecules where the component of the electron orbital angular momentum along the symmetry axis is a constant of motion. For these molecules a rather similar notation of the quantum numbers to that of the atom is used,
e.g. the ground state of molecular oxygen O_2 :

$X^3\Delta_g$

the

X=groundstate;
Δ=the quantum number of the orbital angular momentum projection on symmetry axis (in this case $\Delta=d=|M_L|=2$)
3=triplett, the multiplicity of the resulting spin quantum number (2S+1)
g=parity of the wave functions in homonuclear molecules
(gerade=german for even, as an opposite to ungerade=odd)

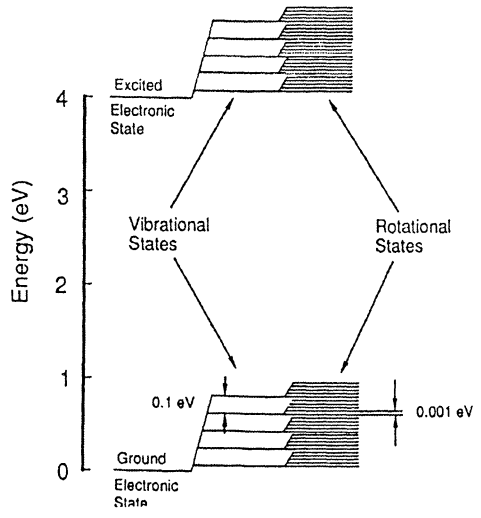

Figure 1.
The relative energy differences between rotational, vibrational and electronic states in a molecule.
(fig. from Svanberg S (1992))

For each electronic state the molecules can also be excited into different vibrational energetic levels which in turn are further split up into rotational energy spectra. These spectra arise naturally from the movement of the nuclei in the molecule.
An electronic transition in the absorption process occurs so quickly, ($\tau \sim 10^{-15} s.$), that the nuclei do not change their relative positions in the rotational-vibrational motion meanwhile, therefore a rapid relaxation to the lowest rotational-vibrational state in the upper level usually follows ($\tau \sim 10^{-13} - 10^{-12} s.$).
The high transition rate of this relaxation depends on the high density of rotational states, according to the relation:

Fermi's golden rule.

The transition rate is:

$$w = \frac{2\pi}{\mathrm{h}}\left|\langle f|H_p|i\rangle\right|^2 \rho(E_i)$$

where $\rho(E_i)$ is the density of the final states.

Once the molecule deexcite it may result in the **emission** of a photon, or through radiationless kinetic interactions with it's environment, sometimes referred to as **internal conversion**. If a photon is emitted the electronic transition can occur to any of the ground level's vibrational-rotational levels and therefore a broad spectrum will be the result, further as the photon has slightly less energy compared to the one that induced the excitation the effect is a red-shift, i.e. the resulting fluorescence spectrum will inevitably be of lower frequency than the excitation light (this shift is named 'Stokes' shift', after the British physicist George Stokes (1819-1903) who discovered fluorescence in fluorite in 1852).

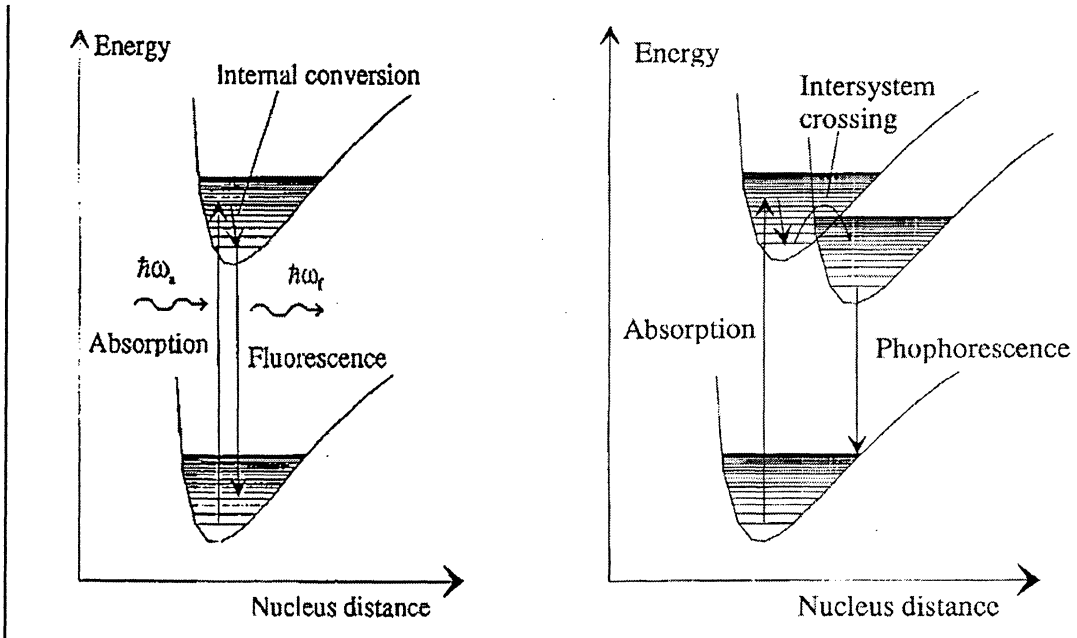

Figure 2.
The diagrams illustrate how the energy levels correspond to spatial reditrubutions of the molecule when interacting with the photons.

According to the selection rules for electric dipole transitions which are predominant if the allowed energy levels exist, the transition to the triplet system is spin forbidden. But all the same it may occur since that description isn't complete, e.g. through collisions as mentioned above. These molecules can be

accumulated in this state for a very long time since the transition to ground state for the same reasons is forbidden, and a much slower transition rate is consequently observed ($\tau \sim 10^{-6} - 1s.$ compared to typically $\tau \sim 10^{-9} - 10^{-8} s.$ in the case of fluorescence).
This process, **phosphorescence**, is less often observed at room temperature.

Naturally several other paths are conceivable; electron transfer, excimer formation, molecular dissociation etc. but for simplicity all competing non-radiative processes will be referred to as **quenching**, with collisional quenching as the most important factor.

In biological samples the most influential quencher is the oxygen molecule which is of great importance as the excited molecule in it's singlett state is a strong toxic agent, which violently oxidises the surrounding tissue if created. Further, as always in biochemistry, the presence of water molecules in the surroundings must be kept in mind. The redistribution of solvent dipoles around the fluorophore and the interaction of hydrogen bonds will additionally contribute to the relaxation process, and in a more thorough description factors as pH, temperature and the environmental polarity must be considered. Not surprisingly the fluorescence spectra from tissues are rather featureless without any characteristic peaks, as the emission of a large number of fluorophores are contributing and because of the other factors mentioned. Perhaps more surprising is, that in spite of this, a lot of important information about the molecules present can be extracted from the spectral profile. In fact, with the use of timegating techniques and with a fair knowledge about the chemical environment it is sometimes possible to determine how chemical changes take place in real time, in e.g. living cells, by studying the spectral entities timeresolved characters.
There is an other very important issue to be solved, - which are the fluorophores in living tissue? By investigating fluorescent materials in nature it becomes clear that the conjugated electron bonds (i.e. every second is a double bond) present in e.g. aromatic hydrocarbons like benzene and naphthalene seems to be the main common feature.

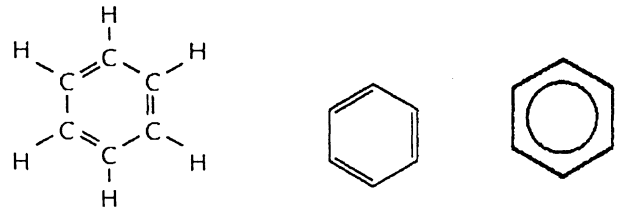

Figure 3.
Benzene, equivalent notations, the rightmost is common and serves as a reminder that the electrons are not possible to locate at any given moment in time.

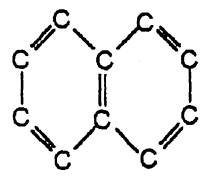

Figure 4.
Naphthalene

As expected only the three aromatic amino acids tryptophan, tyrosine and phenylalanine absorbs light very well but this is enough to make proteins strongly absorbent of UV-light of approximately 280 nm.

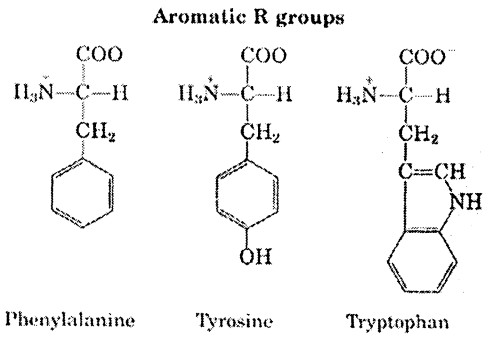

Figure 5.
The three aromatic aminoacids responsible for protein fluorescence.

Some other well known absorbers in nature are chlorophylls, however these considerably larger molecules absorb light in the visible region of the electromagnetic spectrum. The general tendency seems to be that the longer unbroken chain of conjugated double bonds that is present in the molecule the longer is the wavelength
of the peak absorption. This is also in accordance with the 'Hückel approximation' suggesting that only the π-electron that is shared is mobile, further that electron is in a state of resonance with respect to the nearest neighbours to the atom it "belongs to". If one employs variational principal and tries to minimise the total energy for the whole chain theoretically one can show that for the specific oscillation modes that are to be expected, the longer the chain is the lower is the lowest frequency of oscillation, that corresponds to it's minimum energy state.
Nature has a tendency to use only a fraction of the different molecular combinations possible, but in the most disparate functions.
The structure of chlorophylls is a good example of this, if putting a iron ion in the place of the magnesium ion in chlorophyll one has with good resemblance, the prosthetic group of haemoglobin - the heme group.
In both cases the metal ion occupies the central position of a cyclic planar structure called a porypherine ring. The distinct red colour of haemoglobin in blood (and myoglogbin in muscles) is due to the absorbing properties of this ring structure.

Autofluorescence

All mammalian cells have intrinsic fluorescence, autofluorescence, due to the natural presence of fluorescent molecules inside them. Further, there are some of the proteins in the connective tissue that strongly contribute to the tissue fluorescence. It is necessary to have a good understanding of which molecules that are to be expected as naturally present when adding exogenous fluorophores (although higher intensities of excitation light usually is required for autofluorescence to produce detectable emission signals compared to the exogenous molecules).

The excitation, (a), and emission, (b), spectra of pure solutions of endogenous fluorophores, possibly involved in the autofluorescence:

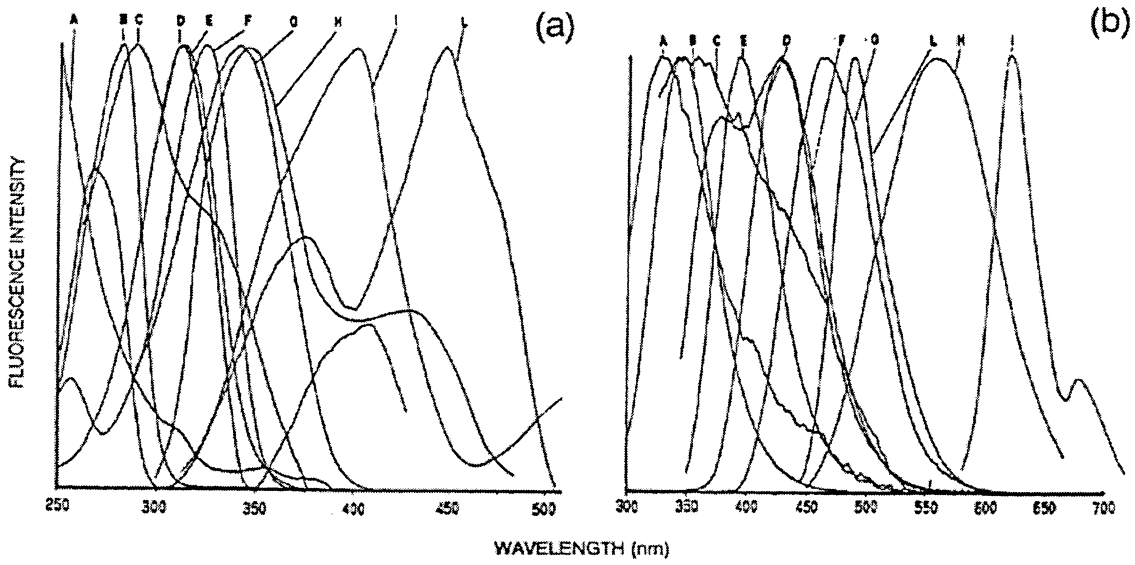

Figure 6.
Spectral shapes are shown for the best relative excitation/emission conditions. All curves are normalised to the peak values. To each fluorophore a fluorescence emission intensity value is presented below in arbitrary units, normalised to the weight of 0.01 mg/ml, exc. 366 nm, em. 380 for collagen, albumin and elastin, but at the emission peak for all the other compounds.

A: collagen	FI = 840	F: 4-pyridoxic acid	FI = 7,960
B: tryptophan-containing proteins, albumin	FI = 26	G: NADH	FI = 950
C: elastin	FI = 64	H: lipopigments (not obtained in this study)	FI = 523
D: pyridoxal-5-phosphate	FI = 22	I: **protoporphyrin IX**	FI = 25,400
L: flavin-mononucleotid	FI = 17,272		
flavin-adenin-dinucleotid	FI = 1,960		

Possibly carotene (with an emission peak ~520 nm) should be added to these graphs, but otherwise these are the fluorophores most frequently mentioned in previous studies. The role of NADH is particularly of interest to the photodynamic therapy application as some experiments suggest that it might serve as one of the primary markers indicating certain modifications in metabolism during the onset and progression of malignant melanomas or even other types of cancers. (Lohman W. -89). During cancer formation an oxidative stress reaction takes place (the agents causing this are still unknown), but since NADH is a strong reducing agent it might help coping with the state. Many studies indicate a substantially higher autofluorescence along the rim of the tumour compared to adjacent healthy tissue (and even less inside the tumour), e.g. (Lohman W., Paul E., 89). It has therefore been concluded that NADH and possibly also its oxidation product NAD could interact with tumour cells,

resulting in cell death (in this model NADH is either incapable of interacting with the surface of intact cell membranes in vivo, or is present in a complex form (with plasma constituents) in healthy tissue, thus inhibiting a deleterious effect). Fortunately, non of the fluorophores mentioned overlaps significantly with the emission spectra of the senstisers investigated in this study.

Photodynamic therapy (PDT).

Photodynamic therapy has been used for some time as an experimental treatment for various malignant tumours. A photosensitising drug, such as porphyrins, is distributed and subsequently the tissue is exposed to irradiation of adequate wavelengths whereby cellular damage and tumour necrosis follows. The cytotoxic effects of PDT are attributed to photochemical reactions mediated by singlet oxygen and other reactive species, as described previously.
Haematoporypherin derivates (HPD) like Photofrin has been used on a clinical basis but a major drawback with this therapy is a generalised cutaneous phototoxicity after systematic administration of HPD that can last up to two months. An alternative method of sensitisation is the topical application of δ-aminoleuvulinic acid (ALA). ALA-induced photosensitisation after topical application is localised to the area of application and resolves within 24 hours (Kennedy, Pottier 1992). Exogenous ALA stimulates the haem biosynthetic pathway which results in endogenous porypherin synthesis of mainly protoporypherin IX (PpIX) in the cancerous cells, probably mainly due to low ferrochelatase activity in the tumour cells and because of effects resulting from the rapid cell proliferation and morphological changes on the histological level in these areas.
The potential for haem production is present, but differently expressed in every nucleated human cell (Kennedy, Pottier 1992, Kennedy et al 1990)
The accumulation of protoporypherin IX is due to bypassing of the negative feedback controls in the haem cycle as a direct result of the excess of ALA present (the translation of mRNA for the syntheses of δ-aminolevulinate synthase is normally feedback inhibited by ALA and the, through saturation and feedback inhibition tightly controlled, mitochondrial enzyme ferrochelatase that combines iron and protoporypherin IX to create haem allows the accumulation of large amounts of intercellular protoporphyrin IX, the lack of iron is also a factor responsible for postponing the formation of new heam molecules).(see Appendix A for further details).

However, there have been reports of lack of selectivity of protoporphyrin IX fluorescence for basal cell carcinoma after topical application of δ-aminolevulinic acid (Alex M.,Whitey D.1995). One explanation to the grossly brighter external protoporypherin IX fluorescence over tumours, in cases of deep tumour lobules of nodular and infiltrating basal cell carcinomas could be that this is due to enhanced penetration through tumour-reactive stratum corneum on the one hand and the greater physical thickness of the tumours compared to the surrounding epidermis on the other. But the absence of reproducible fluorescence marking of nodular and infiltrating basal cell carcinomas suggests that topical ALA may not be a reliable regimen for photodynamic treatment of these tumours.
But once the mechanisms of ALA tumour selectivity are better understood these problems may be solved, therefore studies on the distribution of δ-aminolevulinic acid-induced porphyrins in epidermal tissue and searching for skin agents that can improve ALA penetration into deep lesions might be a significant step towards successful clinical photodynamic treatment of all types of carcinomas.

In the following study ALA is compared to two other tumour marker fluorophores, aluminium phthalocyanine, AlS_2Pc, and benzoporphyrine derivate, BPD, with respect to fluorescence characteristics. ALA has, presumably, the advantage of being less toxic as both ALA and PpIX are naturally present in the human body, albeit not at such high concentrations. There are, however, limited information on the biological effects of the other two substances, and at the present stage they should both be considered potential alternatives to HPD as tumour localisers and sensitisers, (see Appendix A for a chemical description of the substances).

Confocal microscopy

Conventional wide-field light microscopes create images whose effective depth of field at high power is 2-3 μm. Since the resolving power of optical microscopy is about 0.2 μm (the diffraction limitation), superimposition of detail within this plane of focus obscures structurs that would otherwise be resolved. In fluorescence microscopy there is also a problem with light coming from out-of-focus planes when examining objects thicker than the depth of the focal plane. This problems can however be eliminated if using a confocal microscope. A confocal microscope scans a focused spot of light across the specimen and the reflected- or fluorescence light is then collected by the objective lens through a

pinhole aperture to a photomultiplier. Light from out-of-focus planes is not focused on the pinhole and consequently not transmitted to the photomultiplier, hereby the resolution in depth of field is increased down to submicron power.

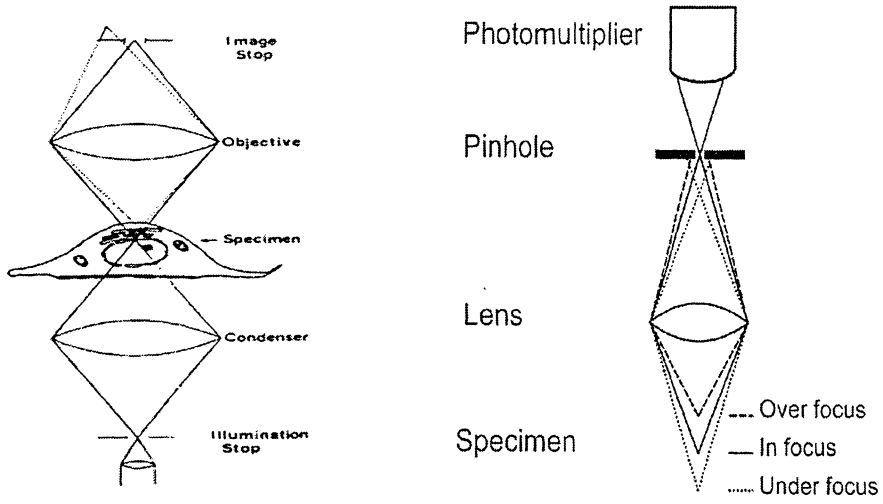

Figure 7.
An illustration of two different confocal arrangements, of which the rightmost could be preferred because of it's relative simplicity in relation to the other and because the detected light must not pass through the entire sample.

By the introduction of well defined resolution in depth it is possible to do 3D-scans of e.g. living cells.
Unfortunately the technique has a few problems to it as well.
As only a fraction of all light is collected through the pinhole, the object must be strongly illuminated. In the case of fluorescence microscopy this means a lot more excitation light which naturally increases photodamage and photobleaching in the sample. Also, the light, supplied by a UV-lamp or by a laser beam, itself have toxic effect on living cells.
Optically, chromatic aberrations as a result of the introduction of a detection pinhole can be a problem as it may cause a dramatic loss of signal. There are three major causes for this; the microscope objective chromatism, influence of the embedding material and depth of object and finally the alignment of the optical system - excitation beam, beam expanders, pin hole - may be imprecise.

Two-photon Excitation Microscopy

Using high power laser light sources gives rise to non-linear optical phenomena. Two-photon absorption is a phenomenon of this kind where the absorption probability depends on the intensity of the incident light to the power of two (i.e. twice the incident intensity yields four times the initial absorption).
The limitations of confocal microscopy can be partially overcome with the help of two-photon excitation microscopy. This comparably new fluorescence microscopy technique offers background rejection in 3D-scanning microscopy as the signal obtained by two-photon excitation is intrinsically restricted to the focal volume of the microscope lens. This very useful property can fairly easily be intuitively understood, whereas the more exact quantum mechanical treatment of the problem is more complex and of less interest to our purposes and is therefore left out (see Appendix B for further details).
The theory of two-photon absorption is similar to that of the scattering of light. Both processes result from the interaction of two photons with one atom - for scattering one is absorbed and the other emitted, whereas for two-photon absorption both are absorbed. Two-photon excitation is the **simultaneous** absorption of two photons that combine their energies to produce an electronic excitation (note the difference to sequential absorption of two photons). The total absorbed energy corresponds to that of one photon with a total energy equal to the sum of the two others. Consider two photons a and b interacting with a molecule. Each of the two photons by itself produces only very small nonresonant oscillations in the molecule as it passes by, at frequency ω_a or ω_b.
If they are both present simultaneously, the oscillation can be thought of as due to the sum and difference frequencies. If $\omega_a + \omega_b$ is a resonant frequency of the molecule, then the small oscillations at that frequency can grow and set up an electromagnetic field that cancels that of the two photons. Thus the two photons are destroyed simultaneously as the molecule is raised to an excited state. Because two photons are required for each excitation the excitation rate depends on the square of the light intensity. Considering the selection rules for dipole transitions one realises that the total parity must remain unchanged ($\Delta S=0, 2$) and therefore the upper state should not be reachable by one-photon excitations.

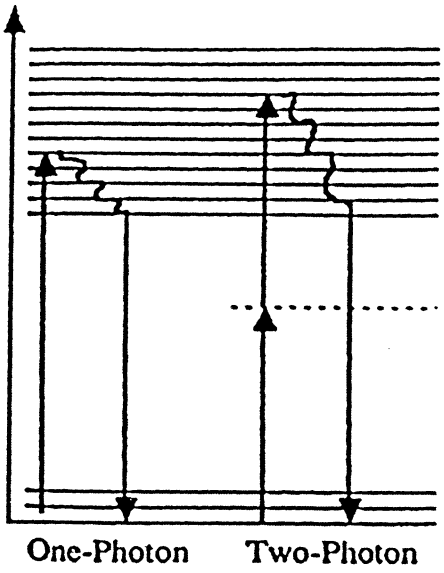

Figure 8.
Despite the fact that one- and two-photon absorption populate different energy levels in the excited state, internal conversion (e.g. vibrational relaxation) to the lowest energy level available causes the fluorescence emission character to be independent of the excitation pathway.

As mentioned above the selection rules are not to be taken too seriously when dealing with complex molecules like biological ones because of the inexactness of the states, and for this reason selection rules will not be taken in to account when dealing with excitation spectra below. However one must keep in mind that differences exist, e.g. tyrosine and phenylalanine, two of the aromatic aminoacids mentioned above are slightly blue-shifted when excited by two-photon absorption (Rehms, Callis 1993), and the general tendency seems to be that symmetrical molecules display this property. The short-lived virtual intermediate state that makes the transition possible is not an actual energy level but it turns out that the presence of real intermediate states close to the virtual state will dictate the transition probability according to;

The transition probability from groundstate g to the final state f is :

$$R_{gf} \propto \sum_i \left| \frac{\langle g|e\vec{r}|i\rangle\langle i|e\vec{r}|f\rangle}{\delta E_i} \right|^2 P^2$$

where the summation is performed over all intermediate states i. δE_i is the energy difference between the virtual and the real intermediate states i, and P is the laser power.
Interestingly, the photon model of light gives a very vivid picture of the process. The probability that a fluorophore will absorb two photons simultaneously depends on both the spatial and temporal overlap of the incident photons (the absorption cross section for one-photon absorption (σ is typically of the order of $10^{-16} cm^2$) is time independent; and the number of excited molecules is equal to the cross section times the excitation intensity ($N_{ex} = \sigma I$). In the case of two-photon excitation the cross section will depend on the spatial extent of the fluorophore and the temporal overlap of the photons, as mentioned above, and is typically of the order of $\delta = 10^{-50} cm^4 s / photon$, assuming that every fluorophore sees the same cross section of the laser, $\sigma = 10^{-16} cm^2$, the photons must arrive within $10^{-18} s$. of

each other as this is the approximate lifetime of the intermediate virtual state, consequently $N_{ex2} = \delta I^2$.

This description is certainly good enough for our means but for the sake of completeness a short summary of the complete description (two photons interacting with a single molecule) follows in Appendix B, although all derivations are omitted;

It is the quadratic dependence of the excitation probability that makes two-photon excitation such a powerful tool in laser scanning fluorescence microscopy, there is no longer a need for a detector pinhole as the signal will come solitary from the focusing volume and consequently the photobleaching will be lessened for the same reason.
The light intensity needed is supplied by subpicosecond mode-locked laser pulses both to minimise temperature damage and to reach sufficiently high light fluxes. The high intensities required was the reason it took 30 years from the theoretical prediction by Göppert Mayer in 1931 until the phenomenon was actually observed. As the invention of the laser was a necessity for any realistic measurements. Nowadays the mode-locked pulsed lasers can reach powers of the order of 10^{12} W and one even has to take into account that too high light fluxes actually can deplete the groundstate and result in saturation even though this is usually avoided.

The scattering processes have a λ^{-4}- (Rayleigh scattering - elastic scattering where the wavelength of the light is larger than the molecular diameter) and λ^{-2}- (Mie scattering - elastic scattering from particles of a size considerably exceeding the light wavelength) dependence, and in this perspective using excitation light of twice the wavelength in two-photon excitations rather then UV-confocal laser scanning spectroscopy can be a great advantage through the improved penetration depth, in e.g. living tissue. But this can, naturally, sometimes be an unwanted effect and the very high intensities required to reach an acceptable level of two-photon absorption leads to photodamage both through heating and by chemical means.
For these reasons the method of excitation should be chosen depending on the experimental situation.

Spatial resolution.

The fundamental principles concerning light distribution and collection in confocal and two-photon excited laser scanning microscopy have been discussed above but the image formation does also strongly depend on the focal geometry. An

illustrative way of discussing this problem is to use the concept of point spread functions (PSF), i.e. the function that describes how an imaging system distorts an ideal point object (mathematically described by the two-dimensional intensity function $\delta(x,y)$, where δ is the dirac distribution). This approach results in the following equations according to (Sako Y. et al. 1997).The intensity PSF in the normalised optical coordinates are the same for both two-photon laser scanning microscopy and the conventional confocal arrangement. But since the unit length in the normalised optical coordinates depends on the wavelength, the spatial resolution in the two-photon case is almost twice as bad as that at hands when using UV confocal technique.

Using normalised optical coordinates (u,v) PSF of the confocal set-up along the focal plane (0,v) and the optical axis (u,0) can be expressed as multiples of PSF of the optics for illumination (I) and the detector (D)

$$PSF_{CLSM}(0,v) = I(0,v)D(0,v)$$

and

$$PSF_{CLSM}(u,0) = I(u,0)D(u,0)$$

where

$$u = (2\pi z n \sin^2\alpha)\lambda_{ex}$$

and

$$v = (2\pi r n \sin\alpha)/\lambda_{ex}$$

r and z are the distances from the focal point along the focal plane and the optical axis, respectively, n is the refractive index of the immersion medium and $n\sin\alpha$ is the numerical aperture of the objective lens. I and D can be expressed as

$$I(0,v) \propto \left[2J(v)/v\right]^2$$

and

$$I(u,0) \propto \left[\sin(u/4)/(u/4)\right]^2$$

$$D(0,v) \propto \left[2J(\beta v)/\beta v\right]^2$$

and

$$D(u,0) \propto \left[\sin(\beta u/4)/(\beta u/4)\right]^2$$

where J_1 is the first order Bessel function and $\beta = \lambda_{ex}/\lambda_{em}$

Since the two-photon laser scanning microscopy is performed without using a detector pinhole, it has no resolution in the detector, and since the excitation

probability of this light is proportional to the square of the illuminating intensity the PSF is;

$$PSF_{2p}(0,v) = I(0,v)^2$$

and

$$PSF_{2p}(u,0) = I(u,0)^2$$

Thus, interestingly, the PSF_{2p} can be improved by introducing a confocal pin-hole at the expense of losing some of the signal if higher resolution is wanted as;

$$PSF_{2p-CLSM}(0,v) = I(0,v)^2 D(0,v)$$

and

$$PSF_{2p-CLSM}(u,0) = I(u,0)^2 D(u,0)$$

The reason these theoretical considerations are of interest in this study is because one of the aims is to calculate the two-photon absorption crossection of the sensitisers investigated. This depends not only on the parameters discussed above, and in Appendix B (one atom and two monochromatic fields), as these larger molecules spatial organisation may contribute greatly to their absorption ability.
In the set-up used in these experiments the detectors are hidden inside the scanning box and hence a direct calculation of the light emitted from a diffraction limited spot as a function of excitation light intensity is complicated by the fact that the detector pin-hole positions and size (the scale is given in arbitrary units) are unknown. A simple way around this problem is to use a fluorophore with a known two-photon crossection and known quantum yield as a reference. For Rhodamine B the crossection, δ has been calculated to $\sim 10^{-50} cm^4$ by assuming that the number of photons pairs absorbed, n_a in each puls in a diffraction limited spot, by the fluorophore when excited with light pulses from a mode locked laser source with average power P_0, wavelength l, and puls width τ_p, with a repetition rate of f_p through a high numerical aperture objective with an NA of A is given by the relation

$$n_a \approx \frac{p_0^2 \delta}{\tau_p f_p^2} \left(\frac{\pi A^2}{hc\lambda} \right)^2$$

where h is Planck's constant, and c is the speed of light in the medium. Knowing the quantum yield of the fluorophore examined a direct comparison is easily done.

Materials and Methods.

Light Sources.

The two-photon process demands very high light intensities to give an acceptable signal to noise ratio. On the other hand the biological samples are sensitive to heat so the average power must be kept low. A pulsed laser supplying very short light pulses at a wavelength where the direct absorption in the sample is limited (low absorption cross-section for one-photon excitation) is a way to fulfil these requirements.
To be able to quantitatively compare the two-photon excited fluorescence to that of ordinary one-photon excited it is necessary to use a laser with roughly half the wavelength of the laser generating the short pulses as a reference.
In these experiments a mode locked Ti:sapphire laser (Coherent MIRA 900), pumped by a continuos Ar^+-laser (Coherent Innova 400), was used supplying ~100 fs. long pulses at a repetition rate of 76 MHz. Due to the very narrow temporal pulsewidth the pulses were spectrally broad, ~ 5 nm, centred around approximately 800 nm. Using a beam-splitter 20% of the average power, ~ 40 mW, was reflected into the microscope's scanning box.
The second laser used was a Kr^+-laser (Coherent Innova 300) supplying continuos light at a wavelength of 406.7 nm. The power of this blue light, entering the microscope's scanning box by an other set of mirrors, was at the time of the experiment ~300 mW.

The Microscope.

The microscope was installed, by Bio Rad microscopy division, just in time for the start of this project. However the very special demands on the system (with both UV, visible and IR excitation light) turned out to have unwanted side effects in diminishing the intensity of the IR as well as the blue light used in this experiment. Only about 3 % of the blue light and 15 % of the IR light remained when the average power was measured just passed the objective lens. The majority of the IR light was lost in the scanning box, consequently it was hard to tell which parts were the most lossy, but there was no problem transmitting the 406.7 nm light.

On the other hand, two dichroic mirrors responsible for splitting off the UV light from the path of the visible light in the module prior to the scanning box (the UV light needs to pass an extra lens packet to compensate for dispersion in the objective lens) transmitted only a fraction of the blue light. By removing the UV correction optics and letting the blue light through the UV path some power was saved. In the system used there were also sets of excitation filters mounted on filterwheels. Some of the pre-installed neutral density filters were used in the experiments, and the optical properties ascribed to these were taken for correct without verification. Purchased with the microscope was a set of filter blocks suited for the various experiments presently conducted at the department, the spectral properties of the ones used in these measurements are graphed in Appendix C.

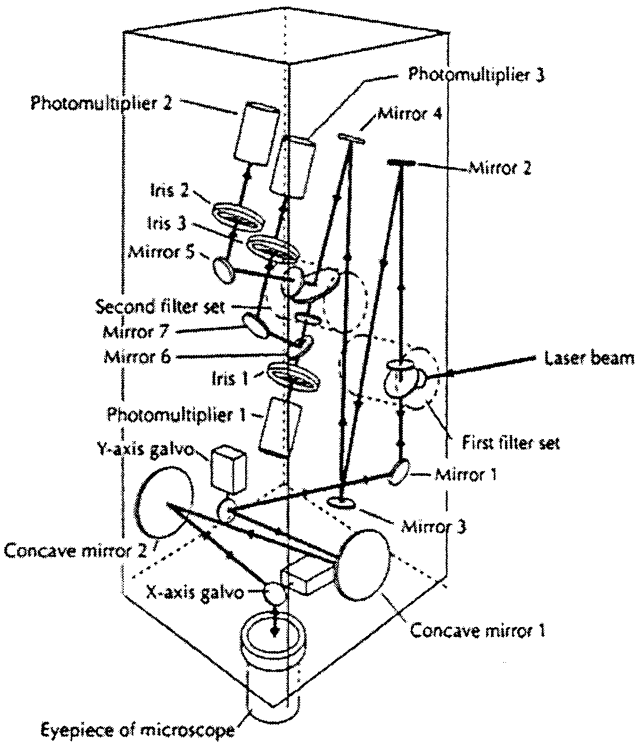

Figure 9.

The scan head, responsible for both transporting the excitation laser beam to the sample, and collecting the fluorescence light supplying it back to the three photomultipliers.
Note that the dichroic mirror (mirror 6) is fixed, reflecting wavelengths above λ=640 nm to PMT3.

Before collecting the fluorescence light in the three photomultipliers there are sets of optional detection filters, these are all mounted inside the scanning box and as in the case with the neutral density filters the transmission profiles given by Bio Rad were considered accurate without further verification (the once used are described in Appendix C).
All the optics mentioned above supported a *Nikon Diaphot 300* inverted microscope when performing confocal laser scanning microscopy, but white light transmission microscopy was also conducted in addition to fluorescence detection as a reference, particularly when examining the tissue specimens.

The 800 nm light pulses.

A first step was to investigate the light sources a bit more thoroughly to make a quantitative comparison of the two methods of excitation possible. For these experiments a conventional *Nikon Labphot-2* microscope was used, equipped with a Plan Apo 10/0.45, a Plan Apo 20/0.75 and a Plan 40/0.70 objective lens. The fluorescence signal was detected with a photomultiplier (Hamamatsu R928). Five dyes with different absorption and emission spectra were chosen (Coumarin 30, Coumarine 503, DCM, Cresyl violet, Rhodamine 6G). The theory states that although the two-photon excitations result in population of other molecular states than the one-photon process, the fluorescence spectrum won't differ greatly in between the two methods, however to fulfil the transition rules the two-photon excitation must sum up to a total change in angular momentum of either 0, -2 or +2. In order to verify this fact a $\lambda/4$-plate was introduced in the light path just prior to entering the microscope, The original IR-light supplied by the Mira was planar polarised and hence could be viewed as a superposition of σ^+- and σ^--light, after passing through the $\lambda/4$-plate the light consisted, ideally, purely of either σ^+- or σ^--light. The particular plate used created a somewhat more elliptically polarised beam at normal incidence (personal communication A. Persson, C-G. Wahlström), so the transformation wasn't complete. Only a very slight drop in the average power (initially 8 mW) reaching the microscope was noticed due to the introduction of the extra piece of glass. As illustrated in Table 1. below the fluorescence signal was altered more markedly. To prove that the reduction of the fluorescence signal wasn't due to stretching of the excitation puls in the extra optical component an objective glass of the same thickness (1 mm) was also put in the same position but this reduced the signal only very little.
An other part of the theory easily verifiable was the quadratic dependence on excitation light intensity. A neutral density filter (NG 5) transmitting ~50% of the incident light intensity was introduced, and a ~75% decrease in fluorescence intensity was noted, accordingly.

Dye:	**2p**	**2p, NG 5**	**2p, $\lambda/4$**	**(a.u.)**
Coumarin 30	7.6	2.0	4.0	
Coumarin 503	8.0	2.0	4.2	
DCM	0.3	0.08	0.16	
Cresyl Violet	0.1	0.03	0.06	
Rhodamine 6G	6.0	1.4	4.4	

Coumarin 30	36.0	9.0	22.0
Coumarin 503	65.0	17.0	32.0
DCM	1.60	0.44	0.90
Cresyl Violet	0.38	0.10	0.28
Rhodamine 6G	54.0	13.5	28.0

Measuring the puls width.

As already mentioned the pulswidth is a critical factor in the process of two-photon excitation. Stretching the puls is an unwanted but inevitable effect of passing it through the system of mirrors and ultimately the objective lens.
It was necessary, both with respect to probing the newly installed system and as a step in the process of quantifying the fluorescence signals to find out to which extent it was broadened. Therefore a scanning autocorrelator (Femtochrome Research In. FR-103XL) was utilised to measure the puls width, before entering, and after passing through the system. The autocorrelator had a conventional Michelson interferometer configuration with a periodic pathlength variation in one of the two light paths induced by two parallel mirrors rotating around a central spindle.

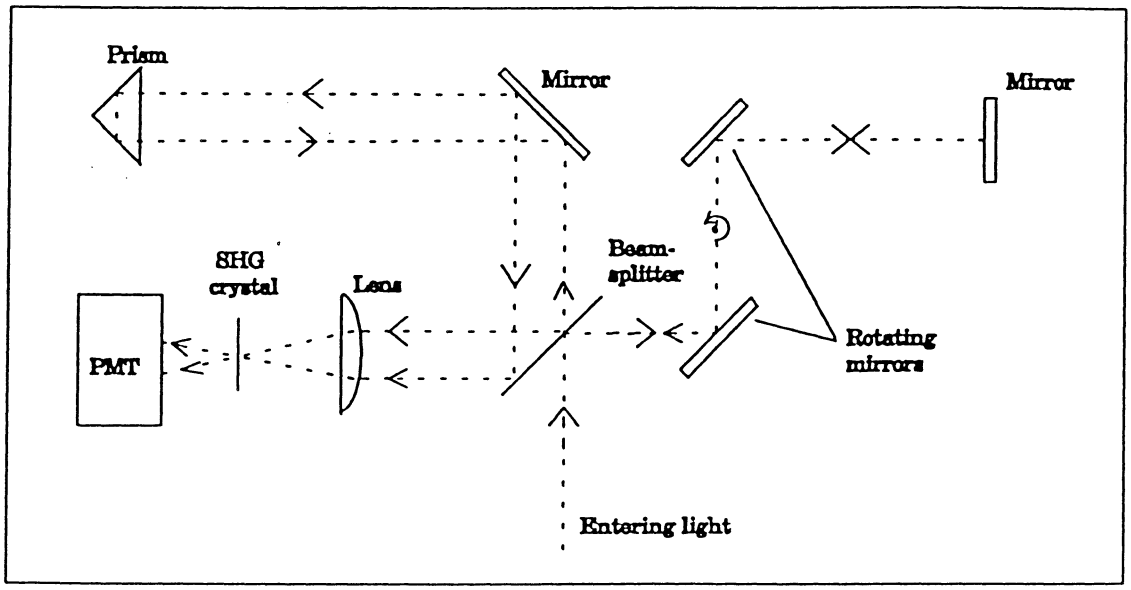

. Schematic of the autocorrelator Femtochrome research inc. FR-103XL..

When the light had past the focal plane a collector lens was mounted just above it to pass transmitted light to the transmission light detector (TLD) placed next to the Hg-lamp used in epi-fluorescence microscopy.

The light pulses were reflected out just after the collector lens, but the beam waist (of the fairly spread-out beam) had to be narrowed using a telescope arrangement (including two additional lenses) before entering the autocorrelator to get a strong enough signal from it's photomultiplier. Consequently the whole measurement came to be more of a worst-case study than an approximate gauging of the puls.

Experimental set-up.

In order to get a good understanding of how the microscope presents scanned images of the samples initial fluorescence information with regard to relative sensitivity of the three photomultipliers, reliability of optical filters, chromatic aberration corrections in objective lenses and effects on spectral entities when introducing a detection pin-hole (confocal microscopy) the transmitted light was collected through an optical fibre (after parking the scanning beam on a domain of interest in the sample), spectrally resolved in a polycromator (SpectraPro-275 Acton Research Corp.) and detected with a CCD-camera (TCCD-5760/RB Princeton Instruments Inc.). The signal was then sent to an EG&G PARC optical multichannel analyser (OMA ST-130) and displayed with help of WinSpec software (TM Princeton Instruments) in graphic form with each channel (the integrated pixel intensity from a column of pixels on the CCD-plate) as a function of wavelength (after appropriate calibration).
In the confocal module each photomultiplier had detection filters and a variable gain, background level and detection iris could be directly adjustaded from the keyboard when acquiring data a 'low signal' function allowed for the photomultiplier to integrate under the maximum amount of time in each pixel depending on the scanning speed.
The only manual measure needed, not performed from the computer program, when changing sources of excitation laser light was the exchange of dichroic filterblocks, although one of the filterblocks (IN2) actually worked well both in the 800 and 407 nm region (see Appendix B for further details). When studying two-photon excitations the irises were kept fully opened (8.0 units), utilising the confocal pin-hole would have improved the spatial resolution (by improving the point spread function) to a theoretical value only ~15% less than the UV confocal resolution with light of half the wavelength (Y. Sako et al.1995). A great deal of the signal would have been lost in this arrangement, and a higher excitation laser power thus would had been needed to get an acceptable signal to noise ratio, and this option seemed less apt to the application of this study where maximum resolution were of no major importance.

In most Kr^+-laser excited measurements the detection filters of the confocal microscope were set to display the reflected excitation light in channel two, the autofluorescence signal in channel one and the signal from the added sensitiser in channel three. When using this filter combination a good correspondence in between the OMA-system's detected signal and the image representation of the microscope was found.

Preparation of samples

Three Whistar/Furth rats that had developed lesions of human adenocarcinoma from colon, were intraperitonealy (i.e directly into the abdomen) given;

1) 100 mg/kg body weight (b.w.) of ALA, (obtained from Porypherin Products, USA), 6h prior to tumour removal.

2) 10 mg/kg b.w. of Benzoporphyrin derivate (BPD), (obtained from Quadra Logic Technologies Inc., Canada), 6-7h prior to tumour removal.

3) 5 mg/kg b.w. of Aluminiumphthalocyanine (AlS_2Pc), (obtained from Porypherin Products, USA), 6-7h prior to tumour removal.

The tumours were frozen to -70 °C immediately after sacrificing the animals and cryo-cutted some weeks later. All the ALA samples were mounted directly on the object glass and the cover glass was attached using transparent nailpolish (along the edges of the coverglass avoiding direct contact with the tissue-sections), whereas half of the BPD- and AlS_2Pc samples were mounted in this same way and the rest of them using a modified embedding substance of p-fenylendiamin dissolved in a phosphate buffered NaCl-solution and glycerine as described in (G.D Johnson & Gloria M de Nogueira Aranjo,1981). The samples were then kept in -20 °C for a period of 1-3 weeks before the experiment. At the time of the experiment five samples were thawed out and stained in two different ways. One sample of each type was stained with hematoxylin and eosin (hematoxylin stains the cell nuclei and other acidic structures blue while eosin stains the plasma red and collagen pink) replacing the first step of dissolving the paraffin normally coating the sections, with a 5 min. wash in formalin and TBS respectively), and two of the ALA samples were stained with alcian blue PAS. The purpose of the first method was simply to facilitate the procedure of identifying histological types in the section, while the second type of staining was meant to selectively stain the adenocarcinoma areas (specifically highly glycocylated regions) in a bright red colour.
All unstained samples were kept well out of light exposure until being examined.

Results and Discussion

To get a qualitative idea of how big the focal volume was when using the confocal pinhole (adjustable irises with a scale ranging from 0.7 to 8.0 units) to discriminate against out of the plane-of-focus fluorescence light, as compared to the intrinsic focusing of the two-photon light supplied to the specimen with wide-open irises, fluorescent beads were used ~16 μm in diameter. Two successive z-scans were recorded (the spacing between adjacent z-sections were approximately 3 μm), one with each type of excitation light, using a 2 unit iris for the 406.7 nm light;

Two-photon image 3

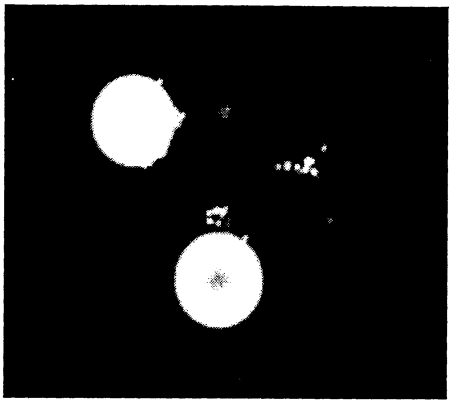

UV image 3

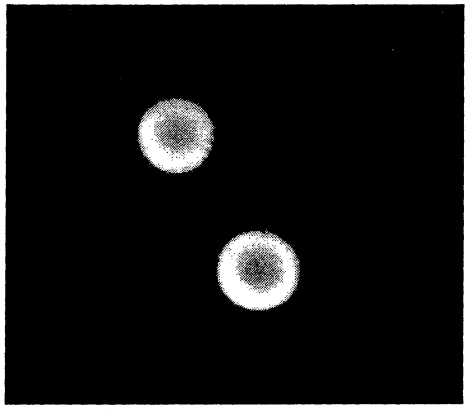

Two-photon image 5

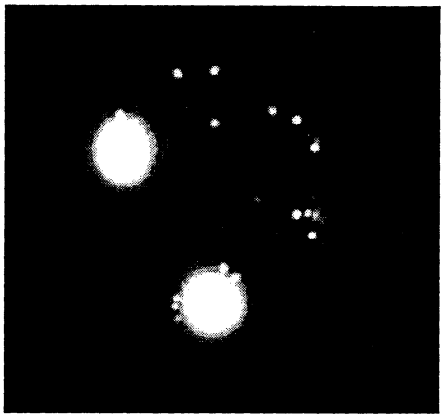

UV image 5

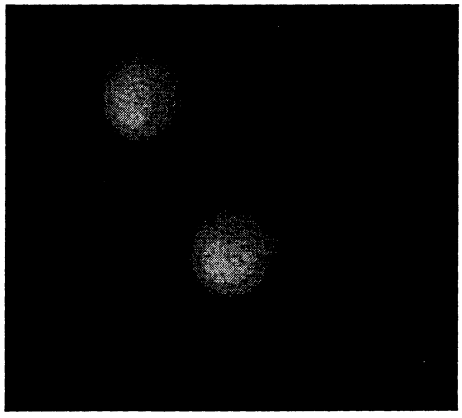

Figure 10.
Two pairs of images selected out of a z-series, the areas displayed are almost identical. They are all detected in channel 3 (640-740 nm). These red beads (spectral profile in Appendix C) turned out to be quite comparable using the two ways of excitation, while the green sort would not yield as much fluorescence intensity when excited with the 800 nm light. The pinhole was set to 2.0 units in the case of UV-excitation and this value gave images restricted in z-direction almost equivalent to the two-photon light source. The mean laser power supplied in the images to the right are about 150 times more than in those to the right and the iris was fully opened. When scanning the plane of focus where the beads are present a significantly stronger signal was detected in the two-photon case as illustrated in the top left picture, while the difference was not as big when comparing the bottom images where the beads are just partly in the plane of focus. Interestingly the salt crystals on top of the cover glass are easily visible when using the 800 nm. excitation as opposite to UV (reflected light was also monitored to make sure no direct scattering was present).

Pulswidth.

The pulswidth was measured applying the set-up described previously.
In figure 12 the original as well as the puls detected after collector lens and telescope are plotted.

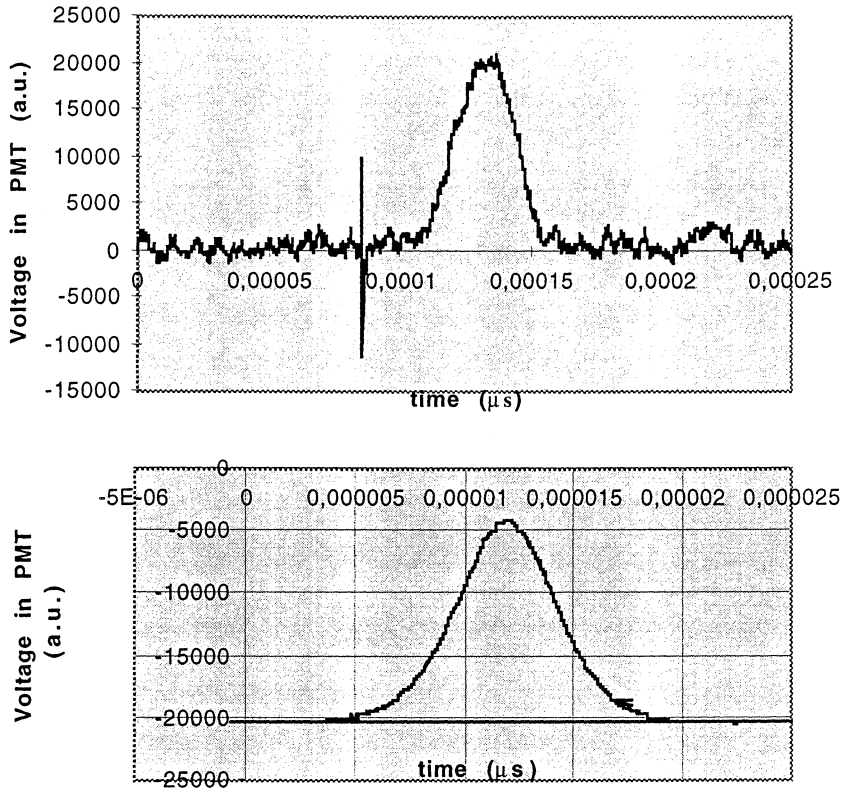

Figure 12.
The initial pulswidth and the width after passing the microscope, the collector lens and an extra telescope arrangement.

The puls reaching the sapmle was approximately 500 fs.
The negative effects caused by the stretching of the puls are not acceptable in a system of this kind, so the current aim must be to localise the parts responsible. The mirrors contribute to a minor extent, the multiple layers the reflected surface is made up of, designed for high reflection in a narrow wavelength band, allows for reflection of the different frequency components making up the puls at slightly different depth as they are not exactly evenly spaced.
Hereby the length of the optical pathway can differ by a few wavelengths, after passing ten mirrors of this kind the temporal spreading is ~200 fs (assuming $\Delta s = 5\lambda$ in each mirror).

According to the relation:

$$n_a \approx \frac{p_0^2 \delta}{\tau_p f_p^2} \left(\frac{\pi A^2}{hc\lambda} \right)^2$$

the signal intensity would hence be only ~1/2 of the optimal.
Also, the puls width directly prior to, and after the scanning box should be measured to ensure that this module does not contain puls stretching elements.

Tumour fluorescence

When examining the fluorescence from the tumour samples, the section next to, or very close to, the stained sample was chosen. Hereby a very close similarity in tissue morphology was ensured. Each sample is presented below with white-light transmission microscopy of the stained sample, the fluorescence detected in channel 3 (640-750 nm) and the complete fluorescence profile in the visible domain. These particular areas were chosen because they contain a boundary between muscle- and tumour-tissue, hence the demarcation specificity of the sensetiser could be tested. The signals detected by the OMA-system were improved considerably by collecting the light from an adjacent area present in all samples were the cryo-cutting procedure had produced an artefact. Parts of the tissue was displaced and the tissue was locally folded in thicker layers resulting in "stripes" with higher fluorescence signal (autofluorescence as well as from the sensetiser, figure 11).

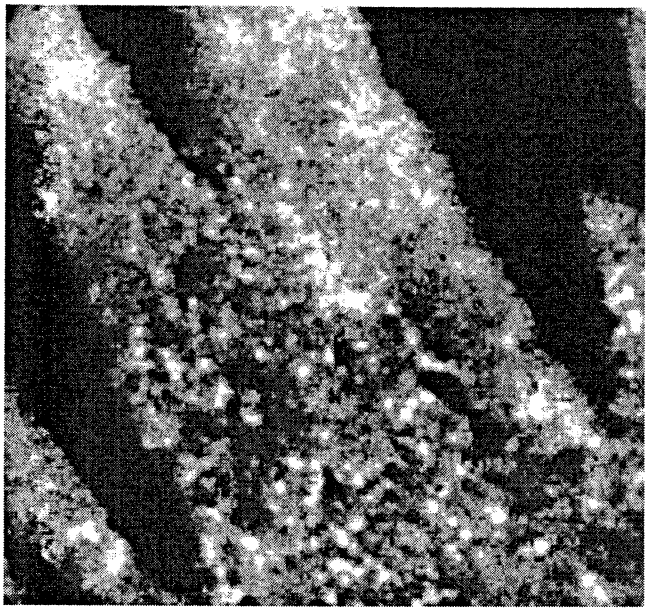

Figure 11
Folded tissue layers gave a strong fluorescence signal, here is channel 3 displayed (mainly sensitiser fluorescence).

The spectral characteristics of this area was however no different to that of the other tumour tissue except for the better signal to noise ratio (a probable explanation could be that there has been a local inflammation due to necrosis of tumour cells, this would have made the area almost fluid and hence caused the artefact when cutting, further the inflammatory reaction could also have altered spectroscopic entities slightly). In the case of BPD the signals were low even when applying this technique and a clean spectrum was not obtained. By using the N_2-laser (λ=337 nm) of the OMA-system the BPD fluorescence peak became stronger, this wavelength seems to be a better choice for excitation of this particular fluorophore. The BPD-graph below was included in spite of the background noise from the computer screen present and the fact that it was recorded before spectral calibration (using a Hg-lamp), as it still gives a hint of the features of the sample's complete spectral profile.
The stained sample photographs reveals the very undifferentiated state of the tumour cells, they exhibit few of the typical characteristics of glandular epithelial tissue found in a histology book, and the alcian blue PAS staining showed no signs of highly glycocylated regions either, which would have been the case under normal circumstances.

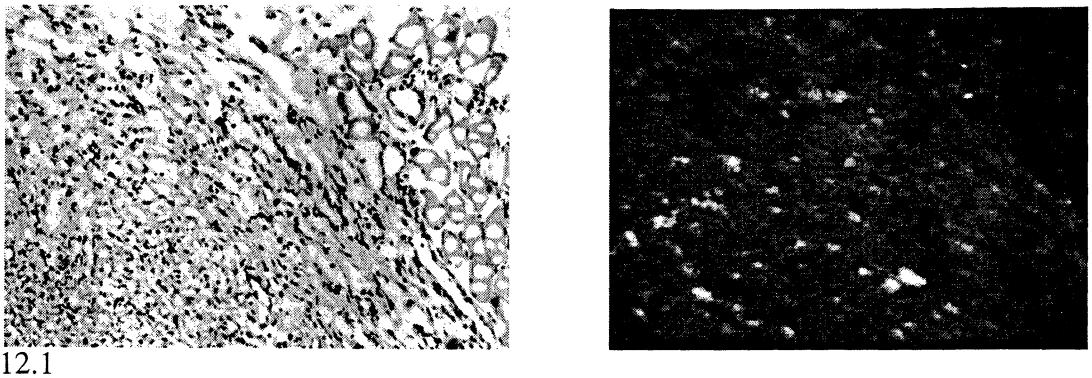
12.1

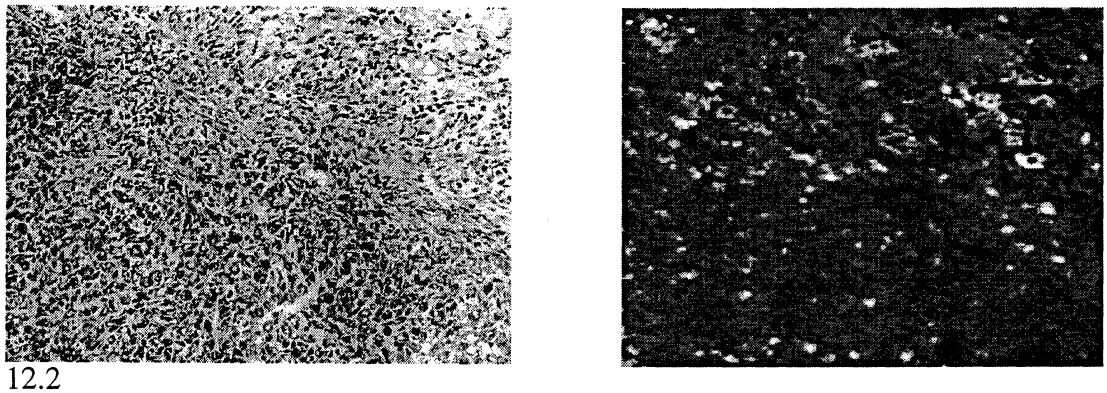
12.2

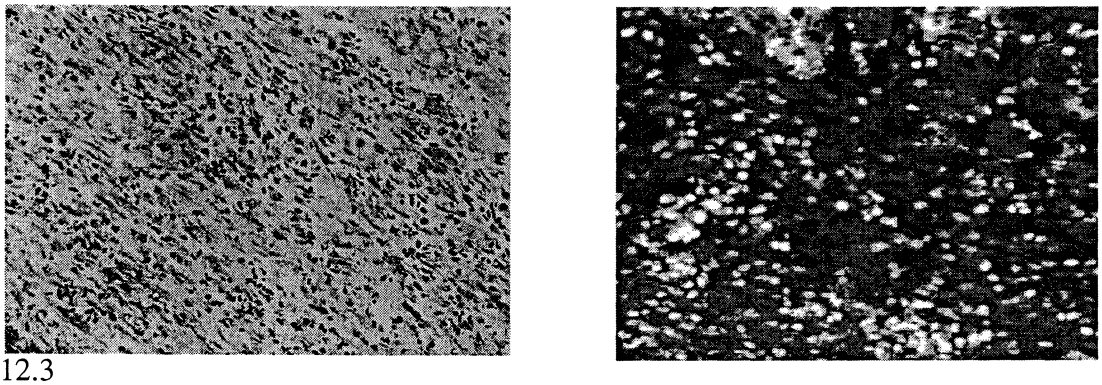
12.3

Figure 12.
The three kinds of photo-sensetisers used displayed with the stained section to the left and the fluorescence detected from a section taken next to the stained one in the tumour to the right.

Further, the muscle cells contain vacuoles, probably caused by the freezing prior to cutting, but can still be identified as the cell-nuclei are clearly located at the rim of each 'bundle' (personal communication U Stenram.). The border between tumour and muscle cells is not very clear due to migration of tumour cells out into the surrounding muscle.

The fluorescence images do not quite display the clear distinction between tumour and healthy tissue that could be expected. One explanation is that the angiogenese may not have been sufficient to supply all parts of the tumour with the chemicals.
The fluorophores seem to be localised mainly intracellulary, in all three cases. The ALA-molecule is small enough to penetrate the cell membrane fairly easily, but the

larger AlS_2Pc and BPD molecules differ greatly with respect to this ability depending on the number of polar groups attached to them, e.g. AlS_4Pc is too polar to be able to pass through the hydrophobic double phosphorlipid layer and consequently localise in the tumour stroma, whereas $AlSPc$ is so hydrophobic that it tends to aggregate and not being distributed properly in *in vivo* studies (Q.Peng et al. (1991)).

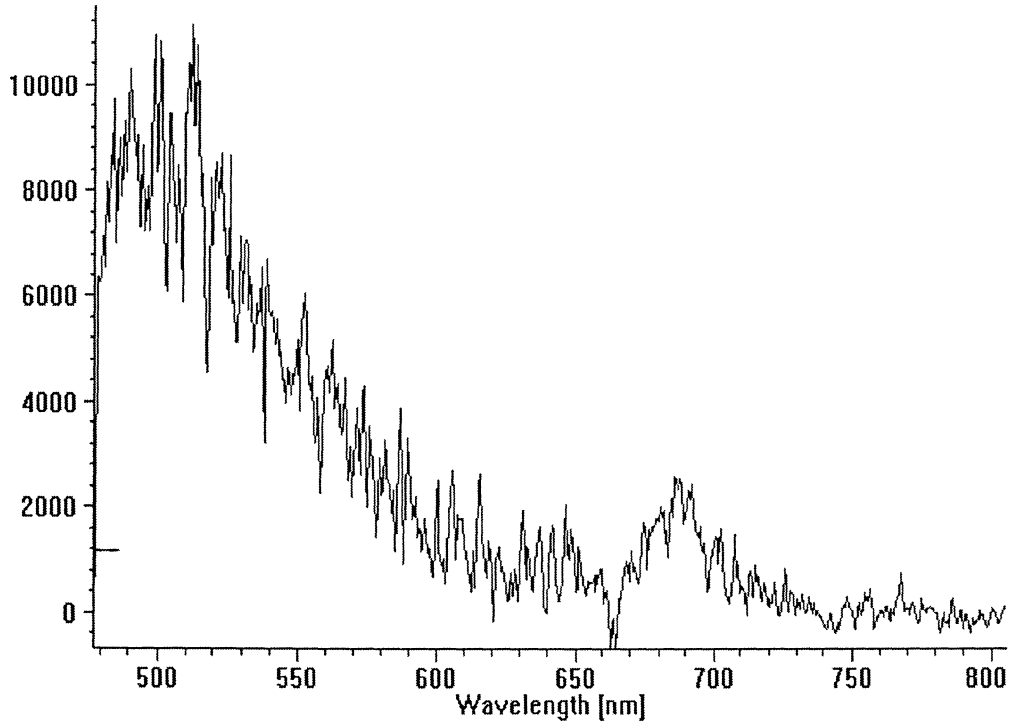

Figure 13.1
AlS_2Pc

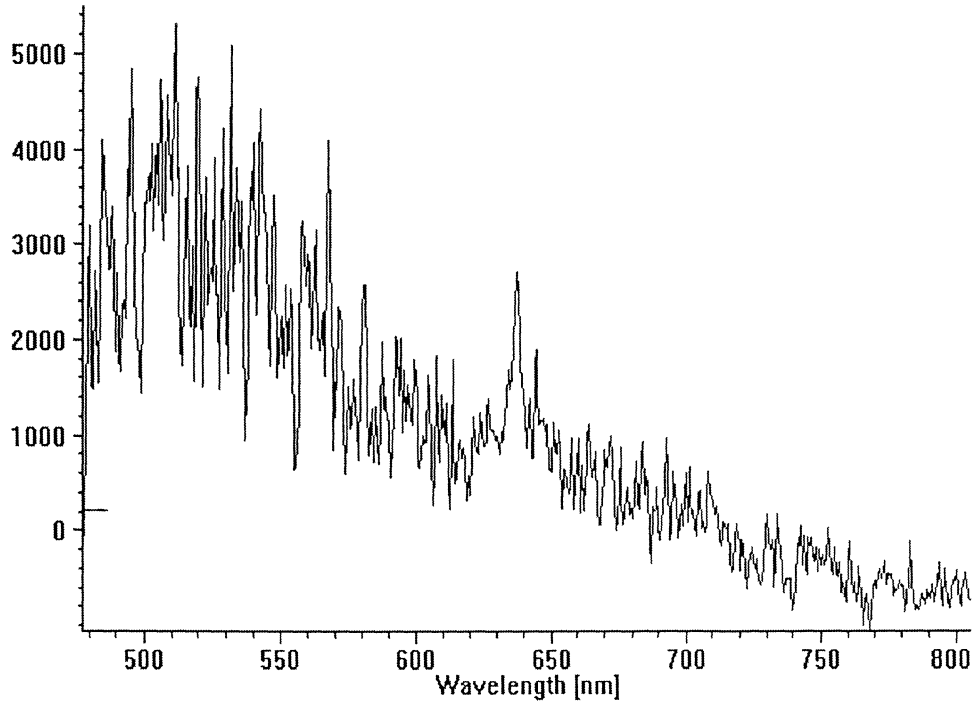

Figure 13.2
ALA

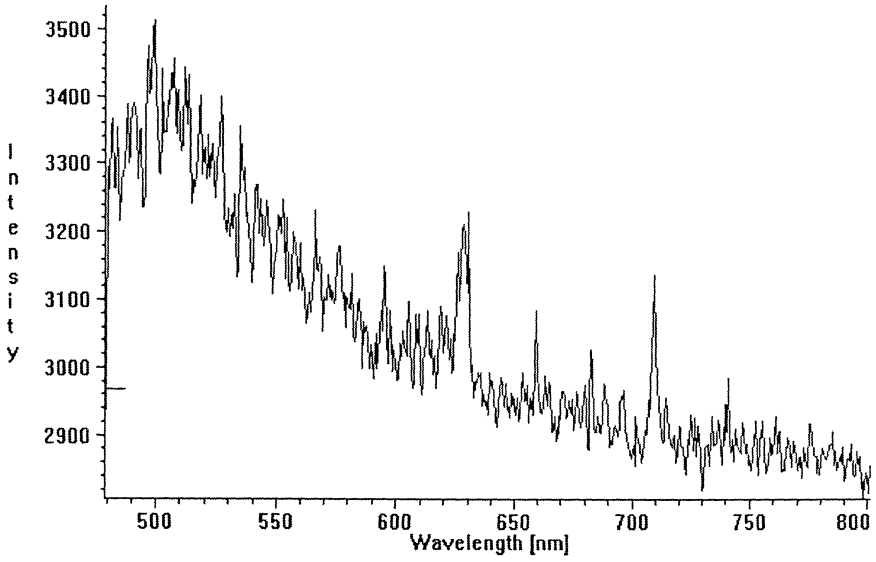

Figure 13.3
BPD
(the peak at 630 nm comes from the computer screen, and the scale is not properly calibrated)

The spectra recorded by the OMA-system confirms the problem with weak signals from the exogenously supplied fluorophores experienced during measurements. The considerably higher light intensity arising from autofluorescence did in many cases coincide with the sensetiser fluorescence. This was not expected and a bit puzzling (autofluorescence is normally not present to any greater extent in the tumour, except for the edges (c.f. above)). However, as the signals from the sensitisers were so weak this abnormality should not be over emphasised, and the fact that the local area where the tissue was folded gave stronger signals over all is not surprising as measurements could not be done with a very small pin-hole (that is these pictures are essentially not confocally restricted in z-level) and therefore the entire multiple layer volume of this area was contributing to the signal detected. The fact that a smaller pinhole wouldn't give strong enough signals can be explained partly by low sensetiser concentrations due to the factors discussed above, but in some of the samples when subtracting an image detected with a smaller pinhole from one taken in the same spot with a some what larger iris resulted in enhancement of sensetiser fluorescence as compared to autofluorescence - this would indicate that the spatial distribution of the two fluorophores differ in that the exogenous one is less concentrated to the centre plane of the section.
But this was not generally the case so further experiments will be needed, preferably with the help of better image processing tools so that images with different irises and from different z-sections easily can be divided.
The images recorded with two-photon excitations were detected with irises fully open, but the signals turned out to be too weak to give any useful information. Except for the problems with the chemicals already mentioned the width of the pulses is certainly a factor that considerably could improve the signals (squeezing the puls down by a factor 5 to it's initial width when reaching the specimen would strengthen the signal by a factor 5).

A very promising trait of two-photon excitaion is the better penetration due to the lower amount of scattered excitation light. In these experiments no thicker samples were examined so this advantage could not be experimentally tested.

An attempt to calculate two-photon crossections.

One current aim for many microscopists is to get means of quantifying the signals detected, particularly in biological systems.
With this in mind an attempt was made to calculate the two-photon cross section of two sensetisers, BPD-MA and AlS_2Pc, similar to the ones used in the experiments described above by comparing the intensity of the fluorescence signal from Rhodamine B. All the substances were solved in ethyleneglycol (3.53 g/l), (BPD with a few drops Dimethylsulphuroxide (DMSO) to improve solubility) and a single drop was placed in between an objective- and a cover glass (the adhesion/cohesion coefficients of the glass plates and the solution did not allow for methanol as solvent). The sample was considered as having essentially no thickness, i.e. the pin-hole size (which actual area wasn't exactly known) in confocal microscopy would not be of major importance.

The TS2 filter block was used in position one as this dicroic was equipped with an extra transmission filter assuring that no reflected excitation light would be detected, in position two the E2 filter block was inserted (this dicroic mirror reflects fairly well around 800 nm despite it's function as low-pass filter in the case of UV excitation and hence it allowed for double checking that reflected light wasn't present and contributing to the detected intensities (transmission profiles in appendix B).
An average power of 23 mW (λ=800 nm) reached the sample applying this set-up. The Fluor 40/0.85 objective with an extra 3X-zooming (restricting the scanned area), the band-pass filter 605/32 in front of PMT1 and band-pass 667/86 for PMT3 was chosen as a suitable filter combination simply by judging the images qualitatively. This selection of filters transmits 570-640 nm light to PMT1 and 640-740 nm to PMT3 Some chromatic aberrations were present (the different channels had slightly different spatial intensity distribution) but when measuring the total intensity the pixel values of the whole fluorescent area was included.
After back ground subtraction the mean pixel value in the selected area was calculated to establish the intensity as compared to that of Rhodamine B. It turned out that the intensity ratio (sensetiser:Rhodamine B) was approximately the same in both PMT:s (the mean value was used in the calculations). As the relative fluorescence, instead of absorption, was tested the results had to be modified in accordance with the fluorophores varying quantum yield.
These efficiencies were estimated to; Rhodamine B: 13 %, AlS_4Pc: 4% and for BPD no value was found so the efficiency of AlS_4Pc was used (the error should not be greater than a factor 2 as this is a typical values of most fluorophores of this kind).

Result of calculation:

$$\delta_{AlS_4Pc} = 3.9 \cdot \delta_{Rhoda\,\min eB}$$
$$\delta_{BPD-MA} = 3.1 \cdot \delta_{Rhoda\,\min eB}$$

$\delta_{Rhoda\,\min B}$ has been measured for λ=1064 nm to be $\sim 10^{-50} cm^4$.
In a very crude approximation one can assume $\delta_{Rhoda\,\min B}$ to differ between 1064 and 800 with the same factor as $\sigma_{Rhoda\,\min eB}$ ($\sigma_{532}/\sigma_{400} \approx 20$) thus $\delta_{AlS_4Pc} \approx 2 \cdot 10^{-51} cm^4$ and $\delta_{BPD} \approx 1.6 \cdot 10^{-51} cm^4$.

This approximation may not be valid as quenching of Rhodamine B appears already at a laser flux of $3 \cdot 10^{27} photons \cdot cm^{-2} \cdot s^{-1}$ (Bradeley D.J. et al (1972)) due to one-photon excitations from the two-photon excited S_1 state to higher states, but this is has yet to be proven in further experiments.

Future Improvements.

The technical difficulties in the first phase of this project were more time consuming than expected still, some details in the very advanced system must be replaced and optimised with respect to the systems various weaknesses before two-photon excited laser scanning microscopy can be performed on low fluorescing objects, e.g. biological samples, with acceptable image quality. In the permanent arrangement 20% of the total power from the 800 nm laser is obtainable corresponding to ~5mW when reaching the sample (the other 80% goes to the high power laser facility applications). But if experiments can be conducted when no other applications are running, 100% can be reflected by simply adding a mirror. Many of the experiments described were therefore made in late evenings. This solution worked well during these experiments, and may be an alternative if the poor transmission efficiency in the optics before the scanning box can not be improved to a reasonable cost. The major draw back is that the UV-correction lens packet that is needed when using ~350 nm excitation light must be taken in and out every time changing from the 351, 353 nm lines to the 407, 413 nm lines of the Kr^+-laser.
As most fluorescence microscopy samples are unstained, phase contrast or differential interference contrast (DIC) white light transmission microscopy is often needed to get an idea of what part of a sample that is currently in the viewing field, at least when dealing with biological samples. This will be possible in the very near future when

prisms for DIC will be purchased. The software supplied by Bio-Rad includes only a minimum of useful image processing tools, by installing a supporting image processing program more advanced analysis can be made.
As the 800 nm beam is too wide to use directly it has to be narrowed with a telescope arrangement, this alignment is, however, very critical for good transmission and the current set-up with two movable lenses should therefore be replaced by a fixed module.
The two-photon signal is dependent on the NA of the objective lens to the power of 4 in the relation used above, this indicates that the NA~1.4 available would improve the signal a factor 10.
To the system will be delivered a monochromator and a streak-camera, to allow for time resolved spectral measurements. This will open many new possibilities of examining microscopic object's spectral behaviour, and this can ultimately also help bridging the gap between the phenomenological biological approach and the chemical description of many processes observed in real world applications.

Acknowledgements.

I would like to thank:

Anders Persson for helping me with pulswidth measurements and computer problems, and Jörgen Carlsson for good advises in the lab. Ingrid Wang-Nordman and prof. Unne Stenram for medical/pathological interpretation of the microscope images included and my tutor Stefan Andersson-Engels for guiding the whole project.

Appendix A. The Photosensetisers used in this study.

1. ALA

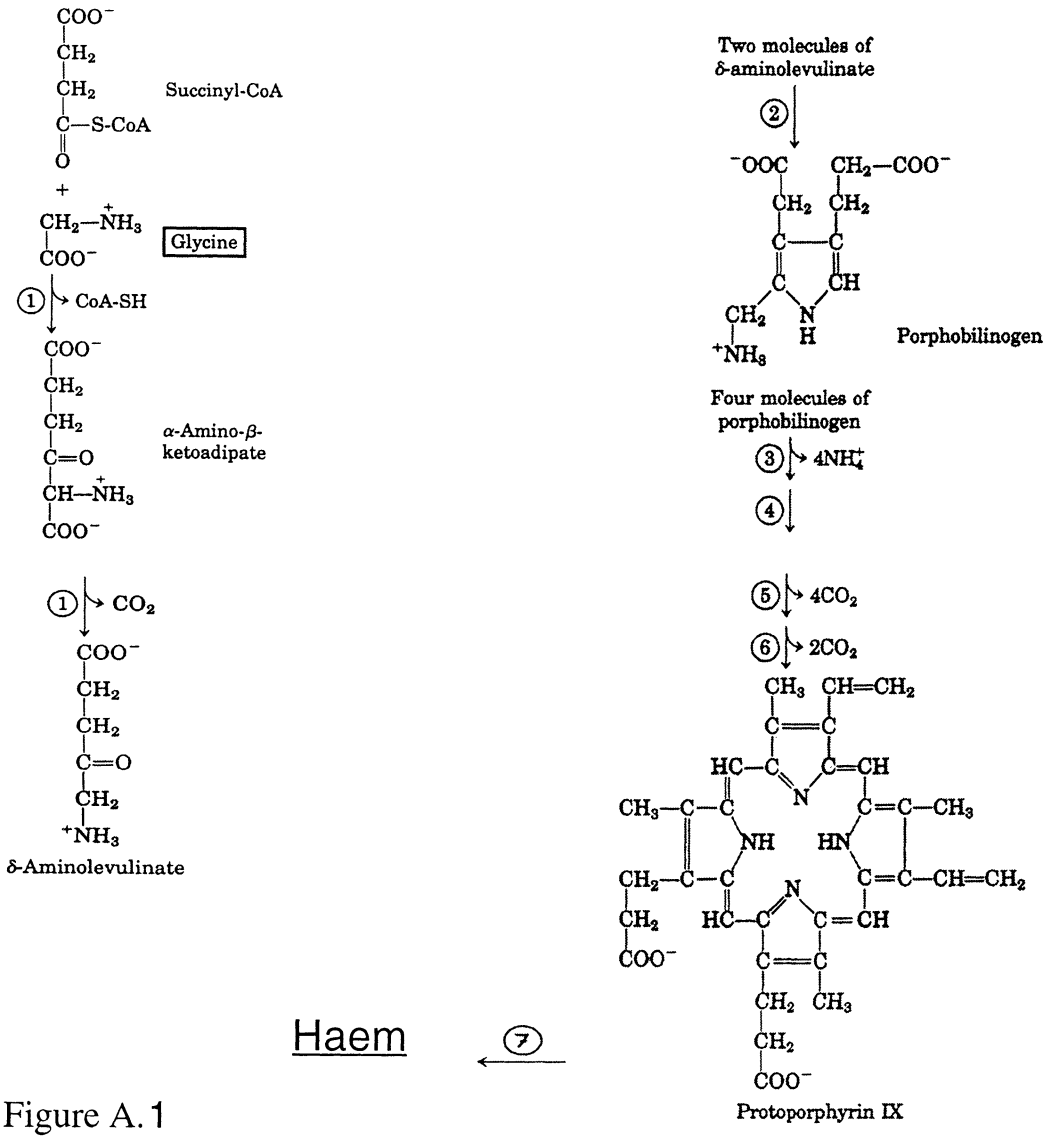

Figure A.1

Biosynthesis of protoporphyrin IX, the porphyrin of hemoglobin and myoglobin, as it occurs in mammals.
The pathway enzymes are:

1. δ-aminolevulinate synthase
2. porphobilinogen synthase
3. uroporphyrinogen synthase
4. uroporphyrinogen III cosynthase
5. uroporphyrinogen decarboxylase
6. coproporphyrinogen oxidase

7. ferrochelatase

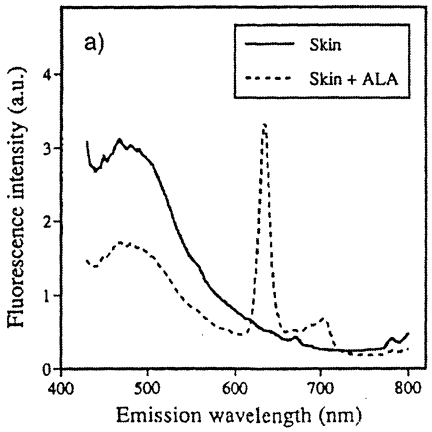

Figure A.2

Appendix B

Two-photon absorption theory

A short description according to (V.I. Bredikhin, M.D. Galanin and V.N. Genkin 1973).
The probability of two-photon transition per unit time in a two level system from state 1 to state 2 under the action of two monochromatic fields (a and b) with frequency ω_a, polarisation vector $\vec{e}_a$, and quantum flux F_a:

$$W_{21}^{ab} = (2\pi)^3 \omega_a \omega_b \left|M_{21}^{ab}\right|^2 \left\{\left[\varepsilon_{aa}(\omega_a)\varepsilon_{bb}(\omega_b)\right]^{1/2} c^2 \mathrm{h}^2\right\}^{-1} F_a F_b \delta(\omega_{21} - \omega_a - \omega_b) \qquad (1.0)$$

$\varepsilon_{aa}(\omega_a)$ is the diagonal component of the dielectric-permittivity tensor in the direction of $\vec{e}_a$ and
M_{21}^{ab} is the composite matrix element;

$$M_{21} = \frac{e^2}{m^2 \omega_a \omega_b} \sum_l \left(\frac{p_{2l}^a p_{l1}^b}{\omega_{l1} - \omega_b} + \frac{p_{2l}^b p_{b1}^a}{\omega_{l1} - \omega_a} \right) \qquad (1.1)$$

where e is the charge and m is the mass of the electron, and p_{21}^a is the matrix element of the component of the momentum operator in the direction of $\vec{e}_a$; l labels the stationary states of the system.
Expression (1.1) is obtained using perturbation theory, if the interaction of the system with the field is chosen in the form

$$V = -(e/c)\vec{A}(t)\vec{p}$$

where $\vec{A}(t)$ is the vector potential of the electromagnetic field.

In these experiments $\omega_a = \omega_b = \omega$.
The $\delta(\omega_{21} - \omega)$ is not strictly a delta function , due to homogeneous broadening of the $|f\rangle$ state it must be replaced with a Lorentzian lineshape,

$$\delta(\omega_{21} - \omega) \rightarrow \frac{\gamma/\pi}{(\omega_{21} - \omega_f)^2 + \gamma^2}$$

where g is a suitible constant depending on if it is collisional broadening or the natural linewidth that is dominating in the experimental set up.

Appendix C. Spectral properties of dicroics and calibration beads.

The spectral fluorescence profile of the red and green 16 mm latex beads.

Red bead

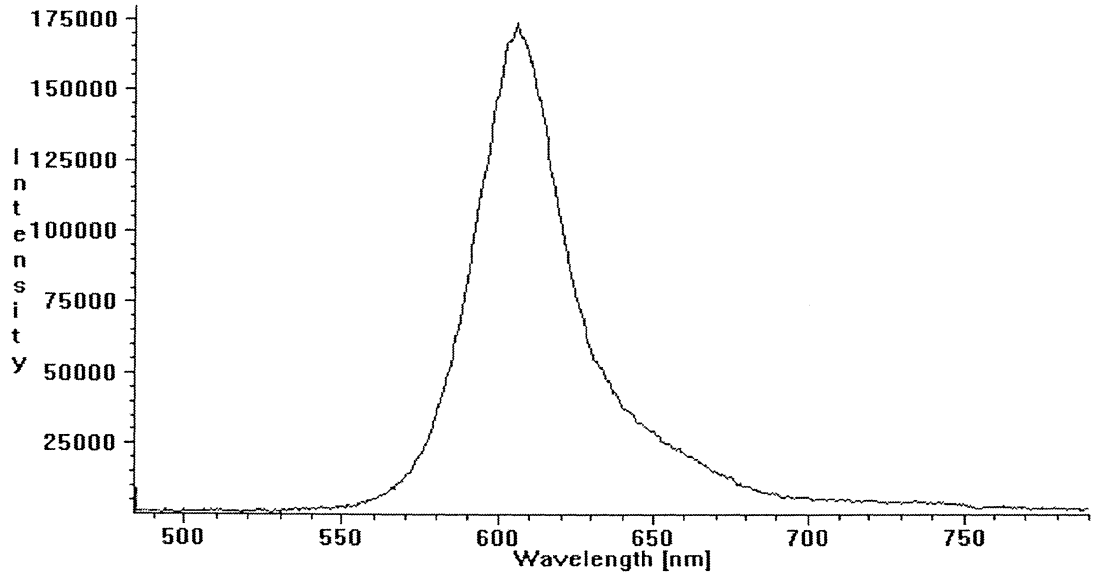

Green bead

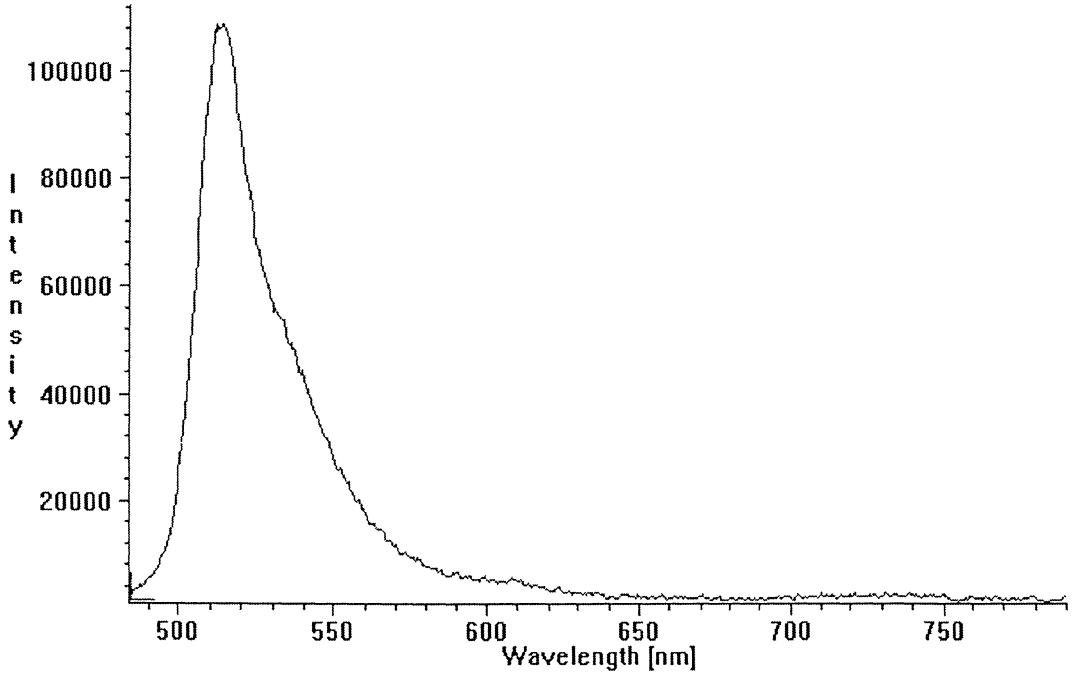

The transmission profiles of the filter blocks.

Referenses.

1. Lehninger A, L., Nelson D. L., Cox M.M., *Principels of Biochemichemistry*. 2 ed. 1993: Worth Publishers.
2. Svanberg S, *Atomic and Molecular Spectroscopy*. 2 ed. 1992, Berlin Hedielberg: Springer-Verlag.
3. Wang X. F, Herman B., *Fluorescence Imaging Spectroscopy and Microscopy*. Vol.137 in Chemical Analysis. 1996, New York: John Wiley & sons, inc.
4. Bredikhin V.I, Galanin M.D., Genkin V.N, *Two-photon Absorption and Spectroscopy.* Soviet-Physics Uspekhi, 1973. **16**(3 Nov-Dec.): 299-321.
5. Johansson J., *Fluorescence Spectroscopy for Medical and Enviromental Diagnostics.* Lund Reports on Atomic Physics LRAP-148, Lund 1993.
6. Johnson G. D. & Gloria M., de Nogueira Aranjo*A simple method of reducing the fading of immunofluorescence during microscopy* Journal of Immunological methods **43**, 349-50 (1981)Elsevier/North Holland Biomedical Press
7. Sako Y., Sekihata A., Yanagisawa Y., Yamamoto M., Shimada Y., Ozaki K. & Kusumi A., *Comparision of two-photon excitation scanning microscopy with UV-confocal laserscanning microscopy in three-dimensional calcium imaging using the fluorescence indicator Indo-1* Journal of Microscopy Vol.185 Pt 1, January 1997 p. 9-20
8. Nakamura O, (1993) *Three-dimensional imaging charecteristics of laser scan fluorescence microscopy:: two-photon excitation vs. single-photon excitation.* Optik, **93**, 39-42
9. Deitche, J., Kempe, M. & Rodolph, W (1994) *Resolution in nonlinear laser scanning microscopy.* Journal of Microscopy **174**, 69-73
10. Stetzler, E.H.K., Hell, S., Lindek, S., Stricker, R., Pick, R., Storz, C., Ritter, G. & Salmon, N. (1994) *Nonlinear absorption extends confocal fluorescence microscopy into the ultra-violet regime and confines the illumination volume.* Opt. Commun. **104**, 223-228
11. Martin A., Tope W.D., Grevelink J.M., Starr J.C, Fewkes J.L., Flotte T.J., Deutch T.F., Anderson R.R Arch Dermatol. Res (1995) **287**, 665-674
12. Kennedy J.C., Pottier R.H (1992) *Endogenous protoporphyrin IX, a clinical useful photosensetizer for photodynamic therapy.* Journal of Photchemistry Photobiology **B 14**: 275-292
13. Kennedy J.C., Pottier R.H., Pross D.C. (1990) *Photdynamic therapy with endogenous protoporphyrin IX.: basic principles and present clinical experience.* Journal of Photchemistry Photobiology **B 6**: 143-148
14. Lohman W., Hugo F.(1989) *The effect of NADH on different human and mouse cell lines.* Naturwissenschaften **76**, 72-74
15. Lohman W.,Paul E. (1989) *Native fluorescence of unstained cryo-sections of the skin with melanomas and nevi.* Naturwissenschaften **76**, 424-426

16. Rehms A.A., Callis P.R. (1993) *Two-photon fluorescence excitation spectra of aromatic amino acids.* Chem. Phys. Lett. **208**, 276-282
17. Bradley D.J., Hutchinson M.H.R., Koetser H., Morrow T., New G.H.C., Petty M.S.(1972) *Two-photon fluorescence quenching and singlet states excitation in Rhodamine dyes.* Proc.R.Soc.Lond.A. **328,** 97-121
18. Bottiroli G., et al.(1995) *Natural fluorescence of normal and neoplastic human colon. A compehensive "ex vivo study".* Lasers in surgery and medicin. 16:48-60